

SimAda: A Simple Unified Framework for Adapting Segment Anything Model in Underperformed Scenes

Yiran Song^{1*}, Qianyu Zhou^{1*}, Xuequan Lu², Zhiwen Shao¹(✉), Lizhuang Ma¹(✉)

© The Author(s)

Abstract Segment anything model (SAM) has demonstrated excellent generalization capabilities in common vision scenarios, yet lacking an understanding of specialized data. Although numerous works have focused on optimizing SAM for downstream tasks, these task-specific approaches usually limit the generalizability to other downstream tasks. In this paper, we aim to investigate the impact of the general vision modules on finetuning SAM and enable them to generalize across all downstream tasks. We propose a simple unified framework called SimAda for adapting SAM in underperformed scenes. Specifically, our framework abstracts the general modules of different methods into basic design elements, and we design four variants based on a shared theoretical framework. SimAda is simple yet effective, which removes all dataset-specific designs and focuses solely on general optimization, ensuring that SimAda can be applied to all SAM-based and even Transformer-based models. We conduct extensive experiments on nine datasets of six downstream tasks. The results demonstrate that SimAda significantly improves the performance of SAM on multiple downstream tasks and achieves state-of-the-art performance on most of them, without requiring task-specific designs. Code is available at: <https://github.com/zongzi13545329/SimAda>.

Keywords Segment Anything Model, Adapter, Underperformed Scenes, Computer Vision, Foundation Models

1 Introduction

Recently, there has been a growing interest in foundation models due to their extensive pre-training on large-scale datasets

* Y. Song and Q. Zhou are joint first authors. Z. Shao and L. Ma are joint corresponding authors.

1 Shanghai Jiao Tong University. E-mail: {songyiran, zhouqianyu, shaozhiwen, lzma}@sjtu.edu.cn

2 La Trobe University. E-mail: b.lu@latrobe.edu.au

Manuscript received: 2024-01-21; accepted: 20xx-xx-xx

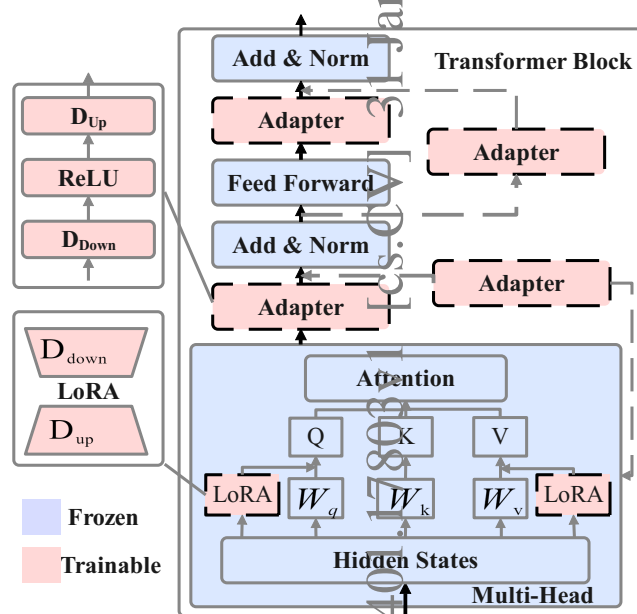


Fig. 1 SimAda: A simple unified framework for adapting SAM in underperformed scenes. SimAda brings trainable parameters, e.g., adapters and LoRA, to different positions of the Transformer backbone in various manners.

and superior generalization capabilities across various downstream tasks. However, in the field of computer vision (CV) [1–5, 5–20], the exploration of foundation models [21–29] is still in its early stage. The pioneering work of CLIP [21] effectively combines image-text patterns and achieves zero-shot generalization. Recently, SAM [22] leverages a single user interface as a prompt to perform object segmentation without additional training. Researchers [23, 30, 30–33] have applied SAM in various real-world scenarios and concluded that SAM exhibits excellent generalization in common scenes but lacks understanding of specialized data. Similar observations have been mentioned in recent studies such as [24–26]. In this work, we use the term “underperformed scenes” to refer to challenging scenarios where SAM’s performance is relatively

unsatisfactory.

Improving the performance of SAM in underperformed scenes is a critical challenge. The most common idea is to perform complete fine-tuning on all model parameters. However, this is computationally expensive for large models in terms of both time and resources. To mitigate this problem, several lightweight alternatives have been proposed [24–26], which only update a small number of additional parameters while keeping the original parameters of SAM frozen. These alternatives that target adapters also introduce task-specific designs that enhance the accuracy of the algorithms. As a result, it can be challenging to attribute the effectiveness solely to the adapters due to the sophisticated designs introduced. There is a lack of in-depth exploration regarding the connections, differences, and impact of these general fine-tuning techniques, as well as how to better leverage their capabilities to other downstream tasks.

In this paper, we propose a simple unified framework called **SimAda**. As shown in Figure 1, our structure is remarkably straightforward, with the red portion inside the dashed box representing the freely selectable modules and the blue portion representing the original SAM structure with frozen parameters. Unlike other methods, we remove all adapter-unrelated operations, such as carefully-designed data augmentation methods, additional auxiliary input information, and post-processing of outputs. This makes our framework a simple and data-agnostic universal framework that can be applied to any visual task dataset.

In our SimAda framework, Adapter and LoRA are regarded as basic design elements, which we unify under the same theoretical explanation. They are both considered modifications to specific hidden states of SAM, enabling the model’s representation space to better align with the feature distribution of particular datasets. Our unified framework decomposes Adapter and LoRA along a shared set of design dimensions and this allows us to transfer design choices across design dimensions to propose new variants.

Based on SimAda, we propose four variants. Unlike traditional adapters, which usually adopt a serial design, our variants encompass parallel and mixed structures. We extensively perform experiments on multiple tasks and datasets, including COD10K [34], CHAMELEON [35] and CAMO [36] for camouflage object detection, ISIC [37] and ColonDBC [38] for medical image segmentation, DUTS [39] for salient object segmentation, SBU [40] for shadow masking, CDS2K [41] for defect segmentation, and DIS-TE4 [42] for complex object shapes.

Through the overall analysis, our SimAda has three following superiorities:

- Significant performance improvements can be achieved by only using SimAda, without additional complex task-specific designs, and these improvements are effective for almost all common visual tasks.
- The position and manner of incorporating Adapter design have been observed to significantly affect the effectiveness. The mixed adapter structure has demonstrated remarkable performance improvements on almost all datasets.
- Surprisingly, the parallel adapter achieves comparable accuracy to the sequential design on multiple datasets. Given the flexibility of the parallel structure, we believe there is significant potential and room for further optimization in this approach.

In this paper, SimAda not only unifies adapters from a theoretical perspective but also explores the impact of different adapter structures on large-scale model fine-tuning. To the best of our knowledge, it is the first time in the field of CV that adapter variants have been proposed under a unified structure and extensively investigated for their impact on SAM architecture. Given the rapid advancement of vision foundational models and their extensive application to downstream tasks, our work provides valuable insights for future researchers to choose appropriate adapter insertion positions and methods based on practical needs.

2 Related Work

2.1 Image Segmentation Task

Image segmentation is a fundamental task in computer vision [43–48]. It involves dividing an image into different regions or segments. Over the years, researchers have proposed various approaches. FCN [49] by Long et al. revolutionized vision segmentation with end-to-end pixel-wise predictions. U-Net [50] by Ronneberger et al. is a popular architecture for biomedical image segmentation. It uses a U-shaped network with skip connections to capture local and global information effectively. Mask R-CNN [51] by He et al. extends the Faster R-CNN framework for object detection by adding a branch for pixel-level mask predictions. DeepLab models [52–54] proposed atrous convolutions and spatial pyramid pooling to improve segment accuracy. In this study, we evaluate SimAda in diverse real-world segmentation applications, including natural images, manufacturing, remote sensing, and healthcare.

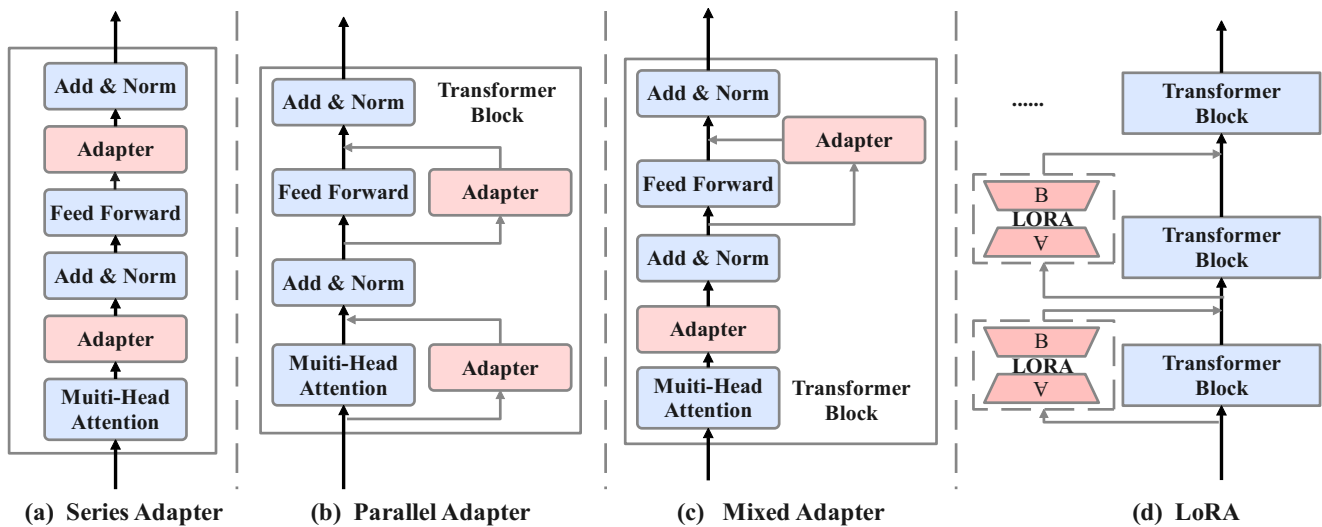


Fig. 2 Illustration of the model architectures of four different the proposed variants, *i.e.*, Series Adapter, Parallel Adapter, Mixed Adapter, LoRA. In this figure, some SAM modules were omitted, and we solely focus on modified components.

2.2 Foundation Models

Foundation models are a new paradigm in artificial intelligence, based on training large neural networks on massive amounts of data using self-supervised learning techniques [55–57]. They learn general representations that can be transferred to different domains and applications. In the field of natural language processing (NLP), models like BERT [58], T5 [59], and GPT [60] have demonstrated impressive performance on a wide range of tasks. Similarly, in CV, foundation models aim to learn universal visual representations from large-scale image-text data. These models, Vision-Language Models (VLM) (CLIP [21] and DALL-E [61]) combine computer vision and natural language processing to understand and generate descriptions or analyze visual content using textual and visual information. Masked Image Modeling [62, 63] (MIM) refers to a technique where parts of an image are masked during training to encourage a model to learn contextual information and complete missing regions. SAM [22] is a model designed for segmenting objects or areas in images, offering precise segmentation capabilities. Previous works mainly focused on improving the accuracy of vision foundation models to specific downstream tasks. In contrast, our approach aims to propose a general solution that enhances the fine-tuning accuracy of vision foundation models across almost all downstream tasks.

2.3 Parameter-Efficient Fine-tuning

Parameter-Efficient Fine-tuning (PEFT) is a technique widely used in the foundation models for both NLP and CV domains. It allows for efficient model adaptation without extensively

modifying the entire network. Two popular methods for implementing this technique are Adapter and LoRA. In NLP, Houshy et al. introduced Adapter-BERT [64], which utilizes lightweight adapter modules to learn task-specific parameters while preserving the pre-trained weights. Pfeiffer et al. proposed Sentence-BERT with adapters [65], which applies adapters to encode sentence embeddings efficiently. In CV, Rebuffi et al. proposed RotNetAdapters [66], which leverages adapters to predict image rotations and enable self-supervised learning. Li et al. introduced Vision-AdapterNet [67], which integrates adapter modules to adapt pre-trained models for image classification. LoRA [68] (Learn Once, Reuse Anywhere) is another approach for parameter-efficient fine-tuning. In NLP, Wang et al. proposed LoRA for BERT [68], which introduces a learnable sparse routing mechanism to share task-specific information across multiple tasks. In CV, [68] introduced LoRA for Vision Transformers, enabling efficient adaptation of pre-trained models for various downstream tasks. Previous works [24–26] typically combine PEFT with other task-specific optimizations for specific domain datasets, making it challenging to truly understand the impact of PEFT design itself on the model. We aim to conduct an in-depth analysis of various PEFT methods and identify straightforward approaches that can better leverage their strengths.

3 Methodology

3.1 Preliminary: Transformer and SAM

Transformer [69] is composed of c stacked blocks, where each block contains two types of sub-module: multi-head self-attention and a fully connected feed-forward network

(FFN). For queries $Q \in \mathbb{R}^{n \times d_k}$ and key-value pairs $K \in \mathbb{R}^{m \times d_k}$, $V \in \mathbb{R}^{m \times d_v}$, the attention maps them as follows:

$$\text{Attn}(Q, K, V) = \text{softmax}\left(\frac{QK^T}{\sqrt{d_k}}\right)V \quad (1)$$

where n and m are the numbers of queries and key-value pairs, respectively, and d_k is the dimension of the tokens. FFN, which consists of two linear transformations with ReLU activation function:

$$\text{FFN}(x) = \text{ReLU}(xW_1 + b_1)W_2 + b_2 \quad (2)$$

where $W_1 \in \mathbb{R}^{d \times d_m}$, $W_2 \in \mathbb{R}^{d_m \times d}$.

SAM [22] consists of an image encoder, a prompt encoder, and a lightweight mask decoder that takes both information sources as input to predict segmentation masks. In this work, we mainly focus on the image encoder module, which is a typical transformer architecture.

3.2 Preliminary: Adapter and LoRA

Inspired by the exploration in the NLP domain by [70], we introduce the basic designs of Adapter and LoRA methods in CV and attempt to derive a unified formulation to establish their connections. Our technical discussion is based on the abstraction of methods [25], [24], and [26], disregarding their designs other than Adapter and LoRA. In our baseline configuration, apart from the additional trainable parameters, the parameters of SAM are frozen. The usage of symbols follows [68] and [70].

The adapter-related method refers to the insertion of small modules between the Transformer blocks. As shown in Figure 1, a general adapter module consists of a down-projection layer $W_{down} \in \mathbb{R}^{d \times r}$, a non-linear activation layer $f(\cdot)$ (typically using ReLU function), and an up-projection layer $W_{up} \in \mathbb{R}^{r \times d}$. Here, “ r ” represents the bottleneck dimension that is significantly smaller than the input dimension. Conventionally (as in [25]), adapter operations are applied sequentially, with one adapter module inserted after the attention layer and another inserted after the FFN layer. These adapters are surrounded by a residual connection. For modules in large model with weight matrix $W_0 \in \mathbb{R}^{d \times k}$ and $h = W_0x$, the final form is:

$$h \leftarrow h + f(hW_{down})W_{up} \quad (3)$$

In our work, as shown in Figure 1, we also explore the parallel implementation of adapters. The adapter operates in parallel with the existing attention layer and FFN, as follows:

$$h \leftarrow h + f(xW_{down})W_{up} + x \quad (4)$$

LoRA [68] hypothesizes the updates to the weights also have a low “intrinsic rank” during adaptation. For a module

with weight matrix $W_0 \in \mathbb{R}^{d \times k}$, LoRA constrains its update by representing the latter with a low-rank decomposition $W_0 + \Delta W = W_0 + BA$, where $B \in \mathbb{R}^{d \times r}$, $A \in \mathbb{R}^{r \times k}$, and the rank $r \ll \min(d, k)$. We consider A as the down-projection layer W_{down} and B as the up-projection layer W_{up} . With $h = W_0x$, it leads to a final form:

$$h \leftarrow h + s \cdot xW_{down}W_{up} \quad (5)$$

and s is the hyperparameter to control the effect of LoRA.

3.3 SimAda with Four Variants

For the similarity between Adapter and LoRA, we propose a unified framework to consolidate existing related works, called **SimAda**. We assume an initial parameter matrix, denoted as W_0 , and original output $h = W_0x$. The parameter matrix that best matches a specific dataset is denoted as W_f , with final output $h_f = W_1x$. Specifically, we cast Adapter and LoRA as learning a residual vector Δh between h and h_f . Throughout the entire fine-tuning process, h and x remain unchanged, and only the residual vector Δh is modified. As shown in Table 1, to better describe this modification process, inspired by the work of [70] in the NLP field, we define a set of dimensions that define different methods as a combinations of instances along these dimensions.

Functional Form is the specific function that computes Δh . We conducted a detailed discussion above and abstracted the Adapter and LoRA into a unified structure of *Down-projection-Nonlinear-Up-projection*. Usually, we use the ReLU function as the non-linear layer.

Insertion Form is how the added module is inserted into the network. We divide it into two types: sequential insertion and parallel insertion.

Modified Location represents the specific module location within the Transformer where the insertion occurs.

Final Function is the final form after the insertion. Based on the proposed SimAda and design elements, we derive four new variants, as shown in Figure 2. Detailed comparisons between these new variants and the original design dimensions are provided in Table 1.

(1) **Series Adapter**: Two adapter modules are inserted between the attention and FFN layers sequentially. (2) **Parallel Adapter**: Similar to (1), we insert two adapter modules, but they are in parallel with the original structure. (3) **Mixed Adapter**: It is a hybrid structure where a serial Adapter is used in the attention layer and a parallel Adapter is used in the FFN layer. (4) **LoRA**: We apply a LoRA structure with a scalar hyperparameter s to the query and value projection layers in the attention module.

Method	Δh	Insertion Form	Modified Location	Final Function
Design Elements				
LoRA	$\mathbf{x}W_{\text{down}}W_{\text{up}}$	parallel	attn key/val	$\mathbf{h} \leftarrow \mathbf{h} + s \cdot \Delta \mathbf{h}$
Adapter	$f(\mathbf{h}W_{\text{down}})W_{\text{up}}$	sequential	ffn/attn	$\mathbf{h} \leftarrow \mathbf{h} + \Delta \mathbf{h}$
	$f(\mathbf{h}W_{\text{down}})W_{\text{up}} + \mathbf{x}$	parallel	ffn/attn	$\mathbf{h} \leftarrow \mathbf{h} + \Delta \mathbf{h}$
Proposed Variants				
Series Adapter	$f(\mathbf{h}W_{\text{down}})W_{\text{up}}$	sequential	ffn/attn	$\mathbf{h} \leftarrow \mathbf{h} + \Delta \mathbf{h}$
Parallel Adapter	$f(\mathbf{h}W_{\text{down}})W_{\text{up}} + \mathbf{x}$	parallel	ffn/attn	$\mathbf{h} \leftarrow \mathbf{h} + \Delta \mathbf{h}$
Mix Adapter	$f(\mathbf{h}W_{\text{down}})W_{\text{up}} + \mathbf{x}$	both	ffn/attn	$\mathbf{h} \leftarrow \mathbf{h} + \Delta \mathbf{h}$
LoRA	$\mathbf{x}W_{\text{down}}W_{\text{up}}$	parallel	attn query/val	$\mathbf{h} \leftarrow \mathbf{h} + s \cdot \Delta \mathbf{h}$

Table 1 Illustration of the design elements and proposed variants of SimAda.

By proposing four variants based on SimAda, we aim to investigate the initial questions: whether these design elements exhibit differences under fair comparison, whether the manner of design element insertion affects accuracy, and whether they excel in different domains for various tasks. In the following sections, we will conduct in-depth discussions and research to address these questions.

4 EXPERIMENTS

4.1 Benchmark Datasets of Different Tasks

Following previous experimental protocol [23], we verify our proposed method on the datasets where SAM underperformed and our method could significantly improve the performance. The selected datasets encompass various downstream tasks, including salient object segmentation [71], complex object shapes segmentation [42], camouflaged object segmentation [34], shadow detection [72], surface defect segmentation [49], and medical field segmentation [38].

Salient object segmentation [71, 86, 87] aims to identify and extract the most visually prominent objects or regions in an image. Accurate salient object segmentation enables the automatic highlighting of important objects, leading to improved image understanding and various downstream applications in CV. **DUTS** [39] is currently the largest salient object segmentation dataset, consisting of 10,553 training images and 5,019 test images.

Complex object shapes [42] refer to objects that exhibit intricate or intricate geometries, often characterized by irregular contours, multiple components, or intricate structures. Complex object shapes pose challenges for computer vision tasks, including object recognition, segmentation, and understanding, as they require advanced algorithms to accurately capture their intricate characteristics and accurately delineate their boundaries. **DIS-TE4** [42] provides 500 highly accurate pixel-level masks for images with complex object shapes. This can evaluate SAM's ability in perceiving boundary details.

Camouflaged object detection [34, 88, 89] is a task that aims

to identify and localize objects that are visually disguised or blended into their surrounding environments. This task poses significant challenges due to camouflage patterns' complex and diverse nature, which often involve color, texture, and shape adaptations. **COD10K** [34] is a substantial dataset specifically designed for camouflaged object segmentation, featuring 10,000 images characterized by similar foreground objects and surrounding. **CAMO** [36] dataset includes 76 images collected from the Internet for testing. **CHAMELEON** [35] consists of 1250 images (1000 images for the training set and 250 images for the testing set).

Shadow detection [40] is a task that involves identifying and distinguishing shadows from the corresponding objects or regions in an image. Shadows can significantly affect image analysis and understanding, as they introduce variations in color, texture, and shape. The goal of shadow detection is to accurately segment and classify shadow regions, enabling applications such as object recognition, scene understanding, and image-based lighting estimation. **SBU** [40] provides carefully annotated shadow masks for 700 images, which is widely used in shadow detection tasks.

Surface defect segmentation [49] aims at identifying and delineating defective regions in an image. It involves automatically detecting and segmenting areas that deviate from the normal appearance, such as scratches, cracks, stains, or other imperfections. Defect segmentation is essential in quality control and inspection processes across various industries, including manufacturing, automotive, electronics, and product packaging. **CDS2K** [41] is a comprehensive concealed defect segmentation dataset, compiled from a variety of established industrial defect repositories. It comprises 2,492 samples, consisting of 1,330 positive and 1,162 negative instances.

Medical Segmentation: ISIC [37] and **ColonDB** [90] are used to verify the generalization capability of SAM in the medical field. The ISIC dataset consists of high-resolution images of skin lesions, along with corresponding ground truth annotations for lesion segmentation and classification.

DUTS [39]			DIS-TE4 [42]			SBU [40]		
Model	Backbone	MAE	Model	Backbone	MAE	Model	Backbone	MAE
VST ₂₁ [73]	T2T-ViT	0.037	Gate ₂₀ [74]	ResNet50	0.109	DSC ₁₈ [75]	VGG-16	0.032
ICONet ₂₂ [76]	ResNet50	0.037	IS-Net [42]	SwinB	0.072	DSDNet ₁₉ [77]	ResNext	0.036
SAM [22]	ViT-B	0.298	SAM [22]	ViT-B	0.373	SAM [22]	ViT-B	0.496
Our SimAda	Para $\Delta diff$	ViT-B 0.055 $\uparrow 24.3\%$	Our SimAda	Para $\Delta diff$	ViT-B 0.080 $\uparrow 29.3\%$	Our SimAda	Para $\Delta diff$	ViT-B 0.234 $\uparrow 26.2\%$
	Series $\Delta diff$	ViT-B 0.148 $\uparrow 15.0\%$		Series $\Delta diff$	ViT-B 0.191 $\uparrow 18.2\%$		Series $\Delta diff$	ViT-B 0.079 $\uparrow 41.7\%$
	Mix $\Delta diff$	ViT-B 0.029 $\uparrow 26.9\%$		Mix $\Delta diff$	ViT-B 0.049 $\uparrow 32.4\%$		Mix $\Delta diff$	ViT-B 0.070 $\uparrow 42.6\%$
	LoRA $\Delta diff$	ViT-B 0.079 $\uparrow 21.9\%$		LoRA $\Delta diff$	ViT-B 0.117 $\uparrow 25.6\%$		LoRA $\Delta diff$	ViT-B 0.180 $\uparrow 31.6\%$
CDS2K [41]			ISIC [37]			ColonDB [38]		
Model	Backbone	MAE	Model	Backbone	MAE	Model	Backbone	MAE
SINetV ₂₂ [78]	Res2Net50	0.102	CASS [79]	CNN+TF	0.086	FAPNet ₂₂ [80]	Res2Net50	0.038
HitNet ₂₃ [81]	PVTv2-B2	0.118	DINO [82]	ViT-B	0.081	CFA-Net ₂₃ [83]	Res2Net50	0.039
SAM [22]	ViT-B	0.611	SAM [22]	ViT-B	0.419	SAM [22]	ViT-B	0.111
Our SimAda	Para $\Delta diff$	ViT-B 0.137 $\uparrow 47.4\%$	Our SimAda	Para $\Delta diff$	ViT-B 0.062 $\uparrow 35.7\%$	Our SimAda	Para $\Delta diff$	ViT-B 0.045 $\uparrow 6.6\%$
	Series $\Delta diff$	ViT-B 0.123 $\uparrow 48.8\%$		Series $\Delta diff$	ViT-B 0.044 $\uparrow 37.5\%$		Series $\Delta diff$	ViT-B 0.031 $\uparrow 8.0\%$
	Mix $\Delta diff$	ViT-B 0.102 $\uparrow 50.9\%$		Mix $\Delta diff$	ViT-B 0.054 $\uparrow 36.5\%$		Mix $\Delta diff$	ViT-B 0.037 $\uparrow 7.4\%$
	LoRA $\Delta diff$	ViT-B 0.165 $\uparrow 44.6\%$		LoRA $\Delta diff$	ViT-B 0.087 $\uparrow 33.2\%$		LoRA $\Delta diff$	ViT-B 0.055 $\uparrow 5.5\%$
COD10K [34]			CAMO [36]			CHAMELEON [35]		
Model	Backbone	MAE	Model	Backbone	MAE	Model	Backbone	MAE
SegMaR ₂₂ [84]	ResNet50	0.034	SINet [34]	ResNet50	0.100	SINet [34]	ResNet50	0.440
SINet [34]	ResNet50	0.092	FBNet [85]	ResNet50	0.081	FBNet [85]	ResNet50	0.032
SAM [22]	ViT-B	0.217	SAM [22]	ViT-B	0.286	SAM [22]	ResNet50	0.334
Our SimAda	Para $\Delta diff$	ViT-B 0.054 $\uparrow 16.3\%$	Our SimAda	Para $\Delta diff$	ViT-B 0.117 $\uparrow 16.9\%$	Our SimAda	Para $\Delta diff$	ViT-B 0.050 $\uparrow 14.1\%$
	Series $\Delta diff$	ViT-B 0.051 $\uparrow 16.6\%$		Series $\Delta diff$	ViT-B 0.108 $\uparrow 17.8\%$		Series $\Delta diff$	ViT-B 0.033 $\uparrow 30.1\%$
	Mix $\Delta diff$	ViT-B 0.025 $\uparrow 19.2\%$		Mix $\Delta diff$	ViT-B 0.070 $\uparrow 21.6\%$		Mix $\Delta diff$	ViT-B 0.033 $\uparrow 30.1\%$
	LoRA $\Delta diff$	ViT-B 0.077 $\uparrow 14\%$		LoRA $\Delta diff$	ViT-B 0.145 $\uparrow 14.1\%$		LoRA $\Delta diff$	ViT-B 0.055 $\uparrow 27.9\%$

Table 2 Quantitative results on applications of (a) salient object segmentation in *common scenes*, (b) salient object segmentation with *highly-accurate details*, (c) shadow detection, (d) concealed industrial defect detection (e) and (f) medical polyp lesion segmentation, (g) (h) and (i) camouflaged object segmentation. Δ shows the performance gaps between SAM and our Methods. We highlighted the best performance values on each dataset.

ColonDB consists of 380 images in total.

4.2 Implementation Details

To ensure a fair comparison, we utilize the same codebase and maintain consistency in training hyperparameter settings unrelated to the methods. We refer to [24], [25], and [26] for guidance. The modifications are solely made to the design dimensions mentioned in Section 3. We uniformly resized the images to 1024*1024 without additional data preprocessing. The structure of all inserted adapters was fixed as shown in Figure 1: a downsampling layer, a ReLU activation function, and an upsampling layer. The hidden dimension was set to 1/4 of the input dimension. All inserted LoRAs were uniformly set with a rank of 4. We used the ViT-B version of SAM

and trained with the BCE loss (Binary Cross-Entropy loss). AdamW [91] optimizer was used for all experiments with an initial learning rate of 1e-4. The StepLR scheduler was employed with a decay step of 10 and a gamma value of 0.5. Fine-tuning was performed for 100 epochs on all datasets. All experiments were conducted on a single NVIDIA GTX 4090 GPU for fair comparisons. The structure of all inserted adapters was fixed: a downsampling layer, a ReLU activation function, and an upsampling layer. The hidden dimension was set to 1/4 of the input dimension.

All inserted LoRAs were uniformly set with a rank of 4. We used the ViT-B version of SAM and trained with the BCE loss (Binary Cross-Entropy loss). AdamW [91] optimizer was used for all experiments with an initial learning rate of 1e-4.

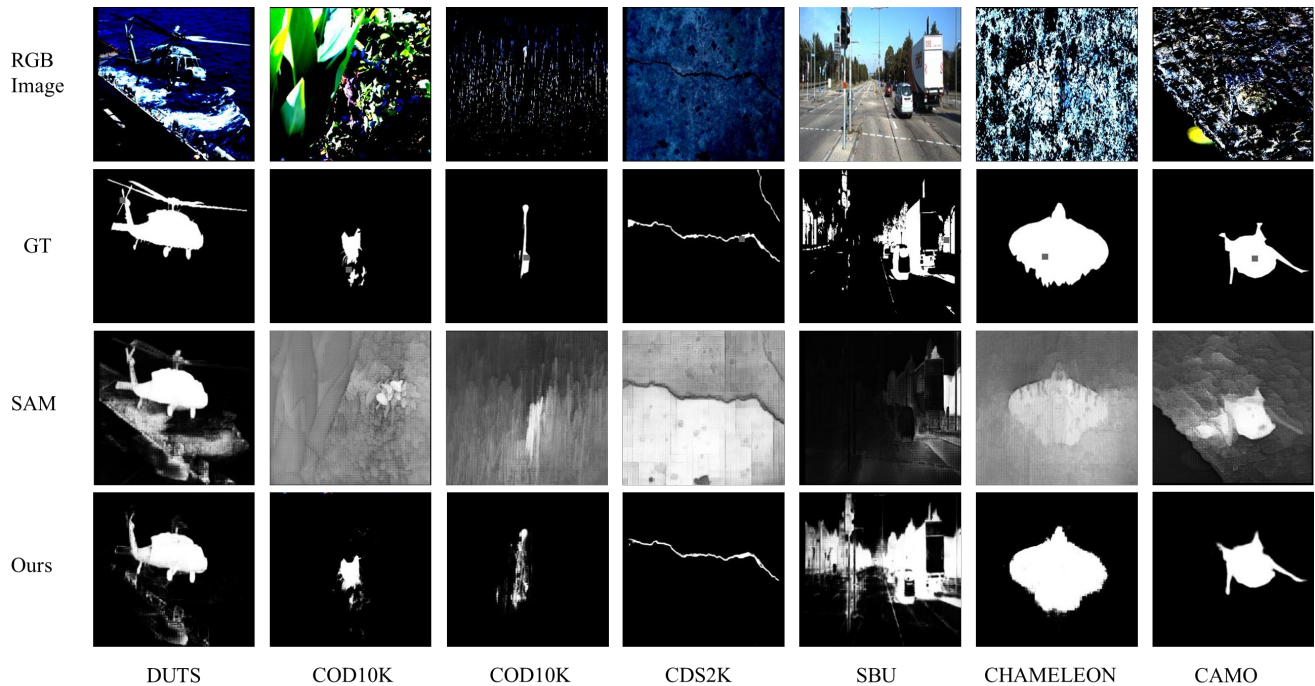


Fig. 3 Visualization results. We randomly selected images from the test sets of several datasets (COD10K [34], SBU [40], DUTS [39], CHAMELEON [35], CAMO [36]). Our method significantly improves the segmentation performance compared to the original SAM.

The StepLR scheduler was employed with a decay step of 10 and a gamma value of 0.5. Fine-tuning was performed for 100 epochs on all datasets. All experiments were conducted on a single NVIDIA GTX 4090 GPU for fair comparisons.

4.3 Main Results

For quantitative evaluation, we employed the widely-used metric: MAE (Mean Absolute Error) score. Lower MAE scores indicate better model accuracy. As shown in Table 2, we compare our four variants with the current SOTA methods on each dataset, as well as SAM (without finetuning) and adapter methods improved specifically for each dataset, to demonstrate the superiority of our approach. From Table 2, we observe that our proposed variants significantly improve the accuracy of SAM on all datasets. For some datasets, our methods achieve similar or even surpass SOTA performance (e.g., COD10K, CAMO, CHAMELEON, DIS-TE4). Among the four variants, Mix Adapter generally achieves the best accuracy. Although adapters are commonly implemented using a sequential structure, our design and experiments demonstrate that parallel structures (Parallel Adapter and LoRA) can achieve superior accuracy compared to sequential structures on several datasets (e.g., DUTS, DIS-TE4). Moreover, the parallel structure allows for a less constrained and more flexible design of the inserted modules, as it is less bounded by the constraints of the original structure. This provides new insights for future researchers in selecting models.

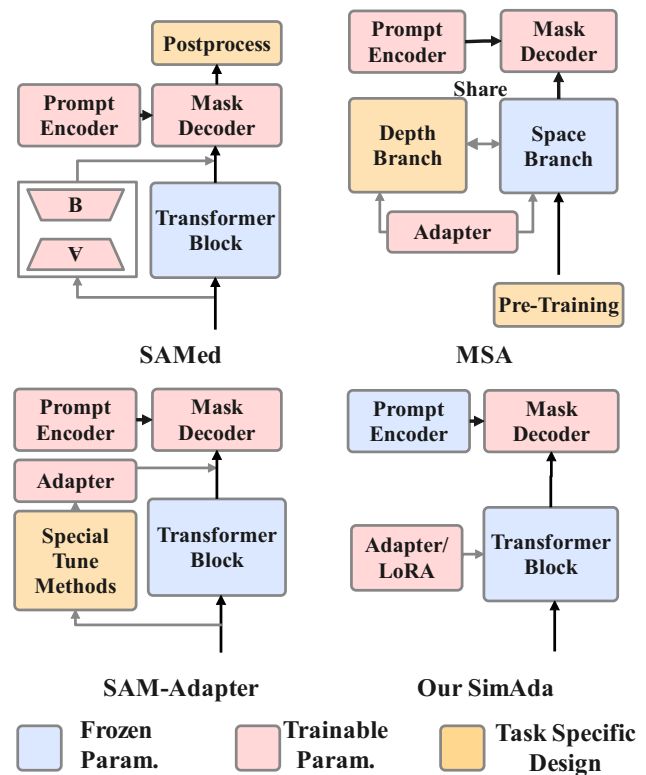


Fig. 4 Architecture comparison with SAM-based adapter approaches [24–26] that introduce task-specific designs.

To further verify the effectiveness of the proposed method, we visualize our segmentation results in Figure 3 that compare

SimAda with the original SAM. Due to space constraints, we randomly selected a subset of images from nine datasets. It can be observed that our approach significantly improves the accuracy of SAM on underperformed scenes. *For more visualization results, please refer to the supplementary material.*

4.4 Discussion on the Differences with Prior Arts

In the methodology, we only discuss the adapter component among all methods, neglecting numerous intricate details of other methods. In this section, we discuss the difference between our SimAda framework with prior arts that are other adapter-based SAM methods. As shown in Figure 4, the blue color indicates the frozen parameters that cannot be trained, the pink color represents the structures that change fine-tuning, and the yellow color represents task-specific designs. Compared to previous works (MSA [24], SAMed [26], SAM-Adapter [25]), we simplify the whole pipeline and the differences lie in the following aspects:

- We do not require additional dataset-specific pretraining. Instead, we keep the original parameters of SAM unchanged and freeze them in the downstream tasks.
- We do not need additional data preprocessing. There is no need for designs similar to SAM-Adapter, which incorporates high-frequency information of the original images as additional input patch embeddings.
- We maintain the original structure of SAM without any modifications, apart from the insertion of the adapter and LoRA. We do not introduce additional multi-scale or multi-branch designs.
- We do not require additional data post-processing. Our input and output remain consistent with the original SAM definition, without employing extra post-processing techniques to enhance model accuracy.

By eliminating these task-specific designs, our model becomes compatible with any dataset, retaining the same level of generality as the original SAM model.

4.5 Efficiency Analysis of SimAda

In practice, when selecting a particular model, the trade-off between accuracy and training cost is often considered rather than focusing solely on accuracy. Table 3 presents a comprehensive analysis of the four variants proposed, taking into account the number of trainable parameters, their proportion to the total parameters of the original SAM model, and training efficiency. Parallel Adapter, Serial Adapter, and Mixed Adapter share the same adapter structure, with only differences in insertion positions, resulting in a similar increase in

Methods	Model Size (M)	Rate	Time (img/s)
Para	10.65M	11.4%	2.64
Series	10.65M	11.4%	2.68
Mixed	10.65M	11.4%	2.58
LoRA	0.15M	0.16%	2.66

Table 3 Effect on the model size and training efficiency of four proposed variants on the DUTS dataset.

the model’s parameter count but with slight variations in training efficiency. In comparison to the adapter method, LoRA variant has significantly fewer parameters, albeit with some accuracy loss. Because all the trainable parameters required by these methods are significantly fewer than the scale of the model itself, they exhibit comparable training speeds. Additionally, the parameter increase introduced by Mix Adapter, relative to the original SAM parameters (accounting for only 11.4%), is deemed acceptable.

4.6 Visualization

Following previous experimental protocol [23], we verify our proposed method on the datasets where SAM underperformed and demonstrate that our method could significantly improve the performance. The selected datasets encompass various downstream tasks, including salient object segmentation [71], complex object shapes segmentation [42], camouflaged object segmentation [34], shadow detection [72], surface defect segmentation [49], and medical field segmentation [38]. To showcase the efficacy of our approach, we present additional visual results as follows in Figure 5 and Figure 6:

5 Conclusion

In this paper, we propose a unified framework called SimAda for adapting SAM in underperformed scenes. Our framework abstracts general modules of different methods into basic design elements, and we design four variants based on a shared theoretical framework. SimAda is research-friendly, efficient, modular, and scalable, which removes all dataset-specific designs and focuses solely on general optimization, ensuring that SimAda can be applied to all SAM-based and even Transformer-based models. Experimental results on nine datasets have demonstrated that all four proposed variants significantly improve the inference performance of SAM on underperformed datasets. The Mix variant stands out with its remarkable performance on almost all datasets, demonstrating competitive results. In addition, although less frequently employed, the parallel architecture design has shown potential on certain datasets. Future work includes integrating new adapters and evaluating them with larger-scale SAM on a wider range of tasks. The code has open-sourced.

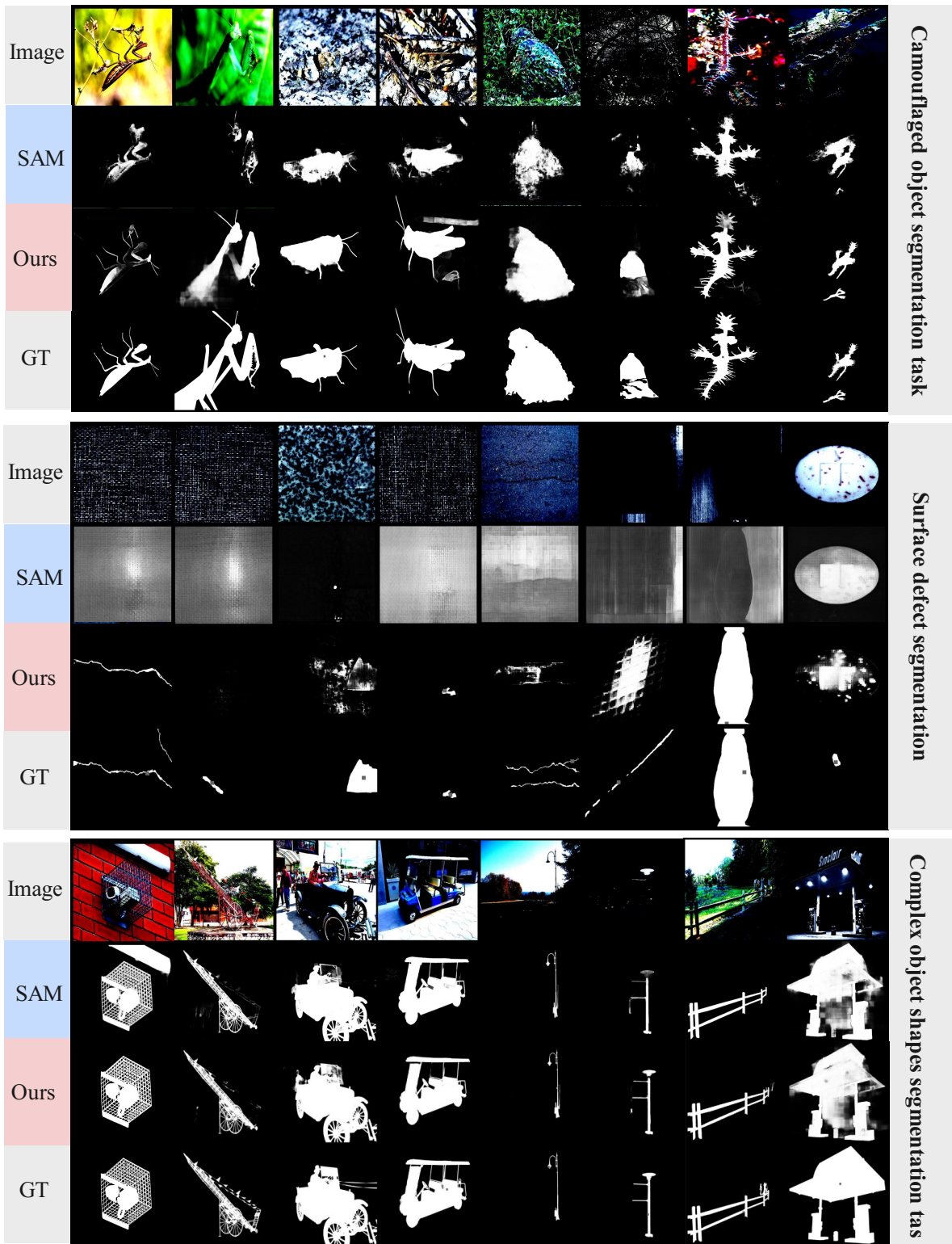


Fig. 5 Visualization results on camouflaged object segmentation, surface defect segmentation, complex object shapes segmentation task.

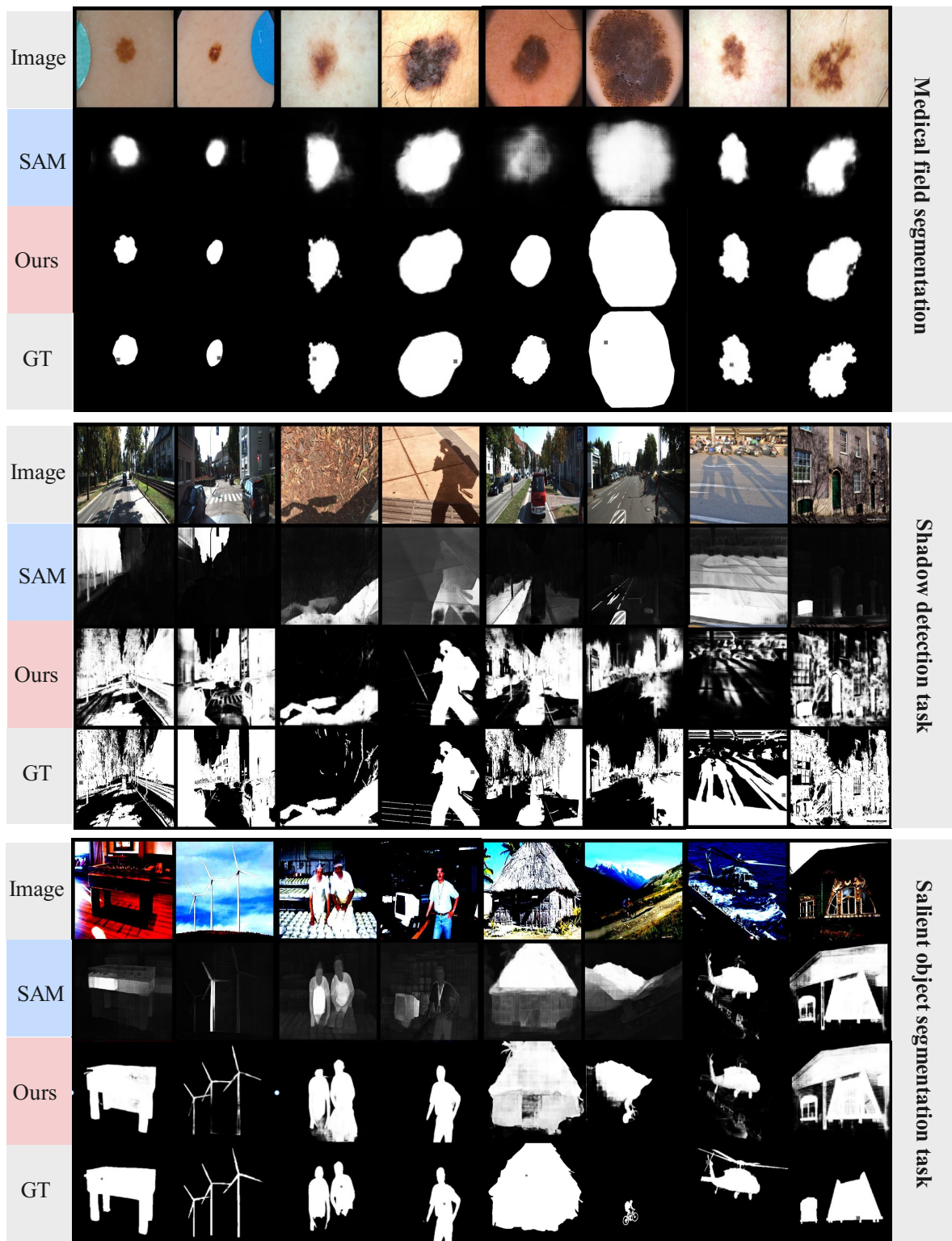


Fig. 6 Visualization results on medical field segmentation, shadow detection task, salient object segmentation task.

References

- [1] He K, Chen X, Xie S, Li Y, Dollar P, Girshick R. Masked Autoencoders Are Scalable Vision Learners. In *CVPR*, 2022, doi:10.1109/cvpr52688.2022.01553.
- [2] Wang X, Girshick R, Gupta A, He K. Non-local neural networks. In *CVPR*, 2018.
- [3] He K, Zhang X, Ren S, Sun J. Deep residual learning for image recognition. In *Proceedings of the IEEE conference on computer vision and pattern recognition*, 2016, 770–778.
- [4] Chen X, He K. Exploring simple siamese representation learning. In *Proceedings of the IEEE/CVF conference on computer vision and pattern recognition*, 2021, 15750–15758.
- [5] Xu H, Liu F, Zhou Q, Hao J, Cao Z, Feng Z, Ma L. Semi-supervised 3d object detection via adaptive pseudo-labeling. In *IEEE International Conference on Image Processing (ICIP)*, 2021, 3183–3187.
- [6] Gu Q, Zhou Q, Xu M, Feng Z, Cheng G, Lu X, Shi J, Ma L. Pit: Position-invariant transform for cross-fov domain adaptation. In *Proceedings of the IEEE/CVF International Conference on Computer Vision (ICCV)*, 2021, 8761–8770.
- [7] Zhou Q, Zhang KY, Yao T, Yi R, Ding S, Ma L. Adaptive mixture of experts learning for generalizable face anti-spoofing. In *Proceedings of the 30th ACM International Conference on Multimedia (ACM MM)*, 2022, 6009–6018.
- [8] Zhou Q, Feng Z, Gu Q, Pang J, Cheng G, Lu X, Shi J, Ma L. Context-aware mixup for domain adaptive semantic segmentation. *IEEE Transactions on Circuits and Systems for Video Technology*, 2022, 33(2): 804–817.
- [9] Zhou Q, Zhang KY, Yao T, Yi R, Sheng K, Ding S, Ma L. Generative domain adaptation for face anti-spoofing. In *European Conference on Computer Vision (ECCV)*, 2022, 335–356.
- [10] Zhou Q, Feng Z, Gu Q, Cheng G, Lu X, Shi J, Ma L. Uncertainty-aware consistency regularization for cross-domain semantic segmentation. *Computer Vision and Image Understanding*, 2022, 221: 103448.
- [11] Zhou Q, Zhuang C, Yi R, Lu X, Ma L. Domain adaptive semantic segmentation via regional contrastive consistency regularization. In *IEEE International Conference on Multimedia and Expo (ICME)*, 2022, 01–06.
- [12] Zhou Q, Gu Q, Pang J, Lu X, Ma L. Self-adversarial disentangling for specific domain adaptation. *IEEE Transactions on Pattern Analysis and Machine Intelligence*, 2023, 45(7): 8954–8968.
- [13] Zhou Q, Li X, He L, Yang Y, Cheng G, Tong Y, Ma L, Tao D. TransVOD: end-to-end video object detection with spatial-temporal transformers. *IEEE Transactions on Pattern Analysis and Machine Intelligence*, 2023, 45(6): 7853–7869.
- [14] He L, Zhou Q, Li X, Niu L, Cheng G, Li X, Liu W, Tong Y, Ma L, Zhang L. End-to-end video object detection with spatial-temporal transformers. In *Proceedings of the 29th ACM International Conference on Multimedia (ACM MM)*, 2021, 1507–1516.
- [15] Zhou Q, Zhang KY, Yao T, Lu X, Yi R, Ding S, Ma L. Instance-Aware Domain Generalization for Face Anti-Spoofing. In *Proceedings of the IEEE/CVF Conference on Computer Vision and Pattern Recognition (CVPR)*, 2023, 20453–20463.
- [16] Feng Z, Zhou Q, Gu Q, Tan X, Cheng G, Lu X, Shi J, Ma L. Dmt: Dynamic mutual training for semi-supervised learning. *Pattern Recognition*, 2022, 130: 108777.
- [17] Song Y, Zhou Q, Ma L. Rethinking Implicit Neural Representations For Vision Learners. In *IEEE International Conference on Acoustics, Speech and Signal Processing (ICASSP)*, 2023, 1–5.
- [18] Long S, Zhou Q, Ying C, Ma L, Luo Y. Rethinking Domain Generalization: Discriminability and Generalizability. *arXiv preprint arXiv:2309.16483*, 2023.
- [19] Long S, Zhou Q, Ying C, Ma L, Luo Y. Diverse Target and Contribution Scheduling for Domain Generalization. *arXiv preprint arXiv:2309.16460*, 2023.
- [20] Guo S, Zhou Q, Zhou Y, Gu Q, Tang J, Feng Z, Ma L. Label-free regional consistency for image-to-image translation. In *IEEE International Conference on Multimedia and Expo (ICME)*, 2021, 1–6.
- [21] Radford A, Kim JW, Hallacy C, Ramesh A, Goh G, Agarwal S, Sastry G, Askell A, Mishkin P, Clark J, et al.. Learning transferable visual models from natural language supervision. In *International conference on machine learning*, 2021, 8748–8763.
- [22] Kirillov A, Mintun E, Ravi N, Mao H, Rolland C, Gustafson L, Xiao T, Whitehead S, Berg AC, Lo WY, et al.. Segment Anything. *arXiv preprint arXiv:2304.02643*, 2023.
- [23] Ji W, Li J, Bi Q, Li W, Cheng L. Segment anything is not always perfect: An investigation of sam on different real-world applications. *arXiv preprint arXiv:2304.05750*, 2023.
- [24] Wu J, Fu R, Fang H, Liu Y, Wang Z, Xu Y, Jin Y, Arbel T. Medical sam adapter: Adapting segment anything model for medical image segmentation. *arXiv preprint arXiv:2304.12620*, 2023.
- [25] Chen T, Zhu L, Ding C, Cao R, Zhang S, Wang Y, Li Z, Sun L, Mao P, Zang Y. SAM Fails to Segment Anything?—SAM-Adapter: Adapting SAM in Underperformed Scenes: Camouflage, Shadow, and More. *arXiv preprint arXiv:2304.09148*, 2023.
- [26] Zhang K, Liu D. Customized segment anything model for medical image segmentation. *arXiv preprint arXiv:2304.13785*, 2023.
- [27] Guo MH, Xu TX, Liu JJ, Liu ZN, Jiang PT, Mu TJ, Zhang SH, Martin RR, Cheng MM, Hu SM. Attention mechanisms in computer vision: A survey. *Computational visual media*, 2022, 8(3): 331–368.
- [28] Ji GP, Fan DP, Xu P, Cheng MM, Zhou B, Van Gool L. SAM Struggles in Concealed Scenes—Empirical Study on” Segment

- Anything". *SCIENCE CHINA Information Sciences (SCIS)*, 2023.
- [29] Cheng S, Ji GP, Qin P, Fan DP, Zhou B, Xu P. Large Model Based Referring Camouflaged Object Detection. *arXiv preprint arXiv:2311.17122*, 2023.
- [30] Song Y, Zhou Q, Li X, Fan DP, Lu X, Ma L. BA-SAM: Scalable Bias-Mode Attention Mask for Segment Anything Model. *arXiv preprint arXiv:2401.02317*, 2024.
- [31] Yin B, Zhang X, Hou Q, Sun BY, Fan DP, Van Gool L. CamoFormer: Masked Separable Attention for Camouflaged Object Detection. *arXiv preprint arXiv:2212.06570*, 2023.
- [32] Huang Y, Yang X, Liu L, Zhou H, Chang A, Zhou X, Chen R, Yu J, Chen J, Chen C, et al.. Segment anything model for medical images? *Medical Image Analysis*, 2023: 103061.
- [33] Wang H, Liu F, Zhou Q, Yi R, Tan X, Ma L. Continuous Piecewise-Affine Based Motion Model for Image Animation. *arXiv preprint arXiv:2401.09146*, 2024.
- [34] Fan DP, Ji GP, Sun G, Cheng MM, Shen J, Shao L. Camouflaged object detection. In *Proceedings of the IEEE/CVF conference on computer vision and pattern recognition*, 2020, 2777–2787.
- [35] Skurowski P, Abdulameer H, B laszczyk J, Depta T, Kornacki A, Kozie l P. Animal camouflage analysis: Chameleon database. *Unpublished manuscript*, 2018.
- [36] Le TN, Nguyen TV, Nie Z, Tran MT, Sugimoto A. Anabranched network for camouflaged object segmentation. *Computer vision and image understanding*, 2019.
- [37] Codella NC, Gutman D, Celebi ME, Helba B, Marchetti MA, Dusza SW, Kallou A, Liopyris K, Mishra N, Kittler H, et al.. Skin lesion analysis toward melanoma detection: A challenge at the 2017 international symposium on biomedical imaging (isbi), hosted by the international skin imaging collaboration (isic). In *International Symposium on Biomedical Imaging*, 2018, 168–172.
- [38] Tajbakhsh Nea. Automated polyp detection in colonoscopy videos using shape and context information. *IEEE Transactions on Medical Imaging*, 2015.
- [39] Wang L, Lu H, Wang Y, Feng M, Wang D, Yin B, Ruan X. Learning to detect salient objects with image-level supervision. In *Proceedings of the IEEE/CVF conference on computer vision and pattern recognition*, 2017, 136–145.
- [40] Vicente TFY, Hou L, Yu CP, Hoai M, Samaras D. Large-scale training of shadow detectors with noisily-annotated shadow examples. In *Proceedings of the European conference on computer vision (ECCV)*, 2016, 816–832.
- [41] Fan DP, Ji GP, Xu P, Cheng MM, Sakaridis C, Van Gool L. Advances in Deep Concealed Scene Understanding. *arXiv preprint arXiv:2304.11234*, 2023.
- [42] Qin X, Dai H, Hu X, Fan DP, Shao L, Van Gool L. Highly accurate dichotomous image segmentation. In *Proceedings of the European conference on computer vision (ECCV)*, 2022, 38–56.
- [43] Zhao H, Qi X, Shen X, Shi J, Jia J. Icnnet for real-time semantic segmentation on high-resolution images. In *Proceedings of the European conference on computer vision (ECCV)*, 2018, 405–420.
- [44] Xiao T, Liu Y, Zhou B, Jiang Y, Sun J. Unified perceptual parsing for scene understanding. In *Proceedings of the European Conference on Computer Vision (ECCV)*, 2018, 418–434.
- [45] Kirillov A, Girshick R, He K, Dollár P. Panoptic feature pyramid networks. In *Proceedings of the IEEE/CVF Conference on Computer Vision and Pattern Recognition*, 2019, 6399–6408.
- [46] Wu H, Zhang J, Huang K, Liang K, Yu Y. Fastfcn: Rethinking dilated convolution in the backbone for semantic segmentation. *arXiv preprint arXiv:1903.11816*, 2019.
- [47] Cheng B, Schwing A, Kirillov A. Per-pixel classification is not all you need for semantic segmentation. *Advances in Neural Information Processing Systems*, 2021, 34: 17864–17875.
- [48] Zhao H, Zhang Y, Liu S, Shi J, Change Loy C, Lin D, Jia J. Psnnet: Point-wise spatial attention network for scene parsing. In *Proceedings of the European Conference on Computer Vision (ECCV)*, 2018, 267–283.
- [49] He T, Liu Y, Xu C, Zhou X, Hu Z, Fan J. A fully convolutional neural network for wood defect location and identification. *IEEE Access*, 2019.
- [50] Ronneberger O, Fischer P, Brox T. U-net: Convolutional networks for biomedical image segmentation. In *International Conference on Medical image computing and computer-assisted intervention*, 2015, 234–241.
- [51] He K, Gkioxari G, Dollár P, Girshick R. Mask R-CNN. *arXiv preprint arXiv:1703.06870*, 2017.
- [52] Strudel R, Garcia R, Laptev I, Schmid C. Segmenter: Transformer for semantic segmentation. In *IEEE International Conference on Computer Vision*, 2021, 7262–7272.
- [53] Chen LC, Zhu Y, Papandreou G, Schroff F, Adam H. Encoder-decoder with atrous separable convolution for semantic image segmentation. In *Proceedings of the European conference on computer vision (ECCV)*, 2018, 801–818.
- [54] Chen LC, Papandreou G, Kokkinos I, Murphy K, Yuille AL. Deeplab: Semantic image segmentation with deep convolutional nets, atrous convolution, and fully connected crfs. *IEEE Transactions on Pattern Analysis and Machine Intelligence*, 2017.
- [55] Bommasani R, Hudson DA, Adeli E, Altman R, Arora S, von Arx S, Bernstein MS, Bohg J, Bosselut A, Brunskill E, et al.. On the opportunities and risks of foundation models. *arXiv preprint arXiv:2108.07258*, 2021.
- [56] Wang X, Chen G, Qian G, Gao P, Wei XY, Wang Y, Tian Y, Gao W. Large-scale multi-modal pre-trained models: A comprehensive survey. *MIR*, 2023.
- [57] Liang PP, Zadeh A, Morency LP. Foundations and recent trends in multimodal machine learning: Principles, challenges, and open questions. *arXiv preprint arXiv:2209.03430*, 2022.
- [58] Devlin J, Chang MW, Lee K, Toutanova K. Bert: Pre-training of deep bidirectional transformers for language understanding. *arXiv preprint arXiv:1810.04805*, 2018.

- [59] Raffel C, Shazeer N, Roberts A, Lee K, Narang S, Matena M, Zhou Y, Li W, Liu PJ. Exploring the limits of transfer learning with a unified text-to-text transformer. *The Journal of Machine Learning Research*, 2020.
- [60] Brown T, Mann B, Ryder N, Subbiah M, Kaplan JD, Dhariwal P, Neelakantan A, Shyam P, Sastry G, Askell A, et al.. Language models are few-shot learners. *Advances in neural information processing systems*, 2020.
- [61] Ramesh A, Dhariwal P, Nichol A, Chu C, Chen M. Hierarchical text-conditional image generation with clip latents. *arXiv preprint arXiv:2204.06125*, 2022.
- [62] Xie Z, Zhang Z, Cao Y, Lin Y, Bao J, Yao Z, Dai Q, Hu H. Simmim: A simple framework for masked image modeling. In *CVPR*, 2022, 9653–9663.
- [63] Liu Z, Hu H, Lin Y, Yao Z, Xie Z, Wei Y, Ning J, Cao Y, Zhang Z, Dong L, et al.. Swin transformer v2: Scaling up capacity and resolution. In *CVPR*, 2022, 12009–12019.
- [64] Houshy N, Giurgiu A, Jastrzebski S, Morrone B, De Larousilhe Q, Gesmundo A, Attariyan M, Gelly S. Parameter-efficient transfer learning for NLP. In *International Conference on Machine Learning*, 2019, 2790–2799.
- [65] Geigle G, Stadtmüller J, Zhao W, Pfeiffer J, Eger S. TUDa at WMT21: Sentence-Level Direct Assessment with Adapters. In *Workshop on Statistical Machine Translation at the Conference on Empirical Methods in Natural Language Processing*, 2021, 911–919.
- [66] Rebuffi S, Bilen H, Vedaldi A. Learning multiple visual domains with residual adapters. In *Advances in neural information processing systems*, 2017, 506–516.
- [67] Hazan A, Shoshan Y, Khapun D, Aladjem R, Ratner V. AdapterNet - learning input transformation for domain adaptation. *arXiv preprint arXiv:1805.11601*, 2018.
- [68] Hu EJ, Shen Y, Wallis P, Allen-Zhu Z, Li Y, Wang S, Wang L, Chen W. LoRA: Low-Rank Adaptation of Large Language Models. In *Conference on Neural Information Processing Systems*, 2022.
- [69] Vaswani A, Shazeer N, Parmar N, Uszkoreit J, Jones L, Gomez AN, Kaiser L, Polosukhin I. Attention is All you Need. In *Advances in neural information processing systems*, 2017, 5998–6008.
- [70] Yu BX, Chang J, Liu L, Tian Q, Chen CW. Towards a unified view on visual parameter-efficient transfer learning. *arXiv preprint arXiv:2210.00788*, 2022.
- [71] Borji A, Cheng MM, Hou Q, Jiang H, Li J. Salient object detection: A survey. *Computational Visual Media*, 2019.
- [72] Hu X, Wang T, Fu CW, Jiang Y, Wang Q, Heng PA. Revisiting shadow detection: A new benchmark dataset for complex world. *IEEE Transactions on Image Processing*, 2021.
- [73] Liu N, Zhang N, Wan K, Shao L, Han J. Visual saliency transformer. In *IEEE International Conference on Computer Vision*, 2021, 4722–4732.
- [74] Zhao X, Pang Y, Zhang L, Lu H, Zhang L. Suppress and balance: A simple gated network for salient object detection. In *Proceedings of the European conference on computer vision (ECCV)*, 2020, 35–51.
- [75] Hu X, Zhu L, Fu CW, Qin J, Heng PA. Direction-aware spatial context features for shadow detection. In *Proceedings of the IEEE/CVF conference on computer vision and pattern recognition*, 2018, 7454–7462.
- [76] Zhuge M, Fan DP, Liu N, Zhang D, Xu D, Shao L. Salient object detection via integrity learning. *IEEE Transactions on Pattern Analysis and Machine Intelligence*, 2022.
- [77] Zheng Q, Qiao X, Cao Y, Lau RW. Distraction-aware shadow detection. In *Proceedings of the IEEE/CVF conference on computer vision and pattern recognition*, 2019, 5167–5176.
- [78] Fan DP, Ji GP, Cheng MM, Shao L. Concealed object detection. *IEEE Transactions on Pattern Analysis and Machine Intelligence*, 2021.
- [79] Singh ea Pranav. CASS: cross architectural self-supervision for medical image analysis. *arXiv preprint arXiv:2206.04170*, 2022.
- [80] Zhou T, Zhou Y, Gong C, Yang J, Zhang Y. Feature Aggregation and Propagation Network for Camouflaged Object Detection. *IEEE Transactions on Image Processing*, 2022.
- [81] Hu X, Fan DP, Qin X, Dai H, Ren W, Tai Y, Wang C, Shao L. High-resolution Iterative Feedback Network for Camouflaged Object Detection. *Proceedings of the AAAI Conference on Artificial Intelligence*, 2023.
- [82] Zhang H, Li F, Liu S, Zhang L, Su H, Zhu J, Ni LM, Shum HY. Dino: Detr with improved denoising anchor boxes for end-to-end object detection. *arXiv preprint arXiv:2203.03605*, 2022.
- [83] Zhou T, Zhou Y, He K, Gong C, Yang J, Fu H, Shen D. Cross-level Feature Aggregation Network for Polyp Segmentation. *Pattern Recognition*, 2023.
- [84] Jia Q, Yao S, Liu Y, Fan X, Liu R, Luo Z. Segment, magnify and reiterate: Detecting camouflaged objects the hard way. In *Proceedings of the IEEE/CVF conference on computer vision and pattern recognition*, 2022, 4713–4722.
- [85] Lin J, Tan X, Xu K, Ma L, Lau RW. Frequency-aware camouflaged object detection. *ACM Transactions on Multimedia Computing, Communications and Applications*, 2023.
- [86] Zhou T, Fan DP, Cheng MM, Shen J, Shao L. RGB-D salient object detection: A survey. *Computational Visual Media*, 2021.
- [87] Ge Y, Zhang C, Wang K, Liu Z, Bi H. WGI-Net: A weighted group integration network for RGB-D salient object detection. *Computational Visual Media*, 2021.
- [88] Zhou T, Fan DP, Chen G, Zhou Y, Fu H. Specificity-preserving RGB-D saliency detection. *Computational Visual Media*, 2023.
- [89] Fan DP, Li T, Lin Z, Ji GP, Zhang D, Cheng MM, Fu H, Shen J. Re-thinking co-salient object detection. *IEEE transactions on pattern analysis and machine intelligence*, 2021, 44(8): 4339–4354.
- [90] Tajbakhsh N, Gurudu SR, Liang J. Automated polyp detection in colonoscopy videos using shape and context information. *IEEE Transactions on Medical Imaging*, 2015.

- [91] Loshchilov I, Hutter F. Decoupled Weight Decay Regularization. In *International Conference on Learning Representations*, 2018.